Solar Energy
And Sustainable Development
Refereed, biannual scientific journal issued by:
The Libyan Center for Solar Energy Research and Studies

Robust Control for DFIG-Based WECS with ANN-Based MPPT

Achraf El Ouali [1*], Yassine Lakhal [2], Mohamed Benchagra[3], Hamid Chojaa[4], Mohamed Vall Ould Mohamed[5].

[1,2,3]Team of engineering and applied physics Higher school of Technology of Beni Mellal, Morocco.
[4]Higher School of Technology, Sidi Mohamed Ben Abdellah University, Fez 30000, Morocco.
[5]Department of Computer Engineering and Networks, College of Computer and Information Sciences, Jouf University, Sakaka 75471, Saudi Arabia.
[1,2]The Moroccan Asociation of Sciences and Techniques for Sustainable Development (MASTSD), Beni Mellal, Morocco.

E-*mail:* [1]elouali.hraf@gmail.com ,[2]lakhal.yassine.doc@gmail.com ,[3]m.benchagra@gmail.com , [4]hamid.chojaa@usmba.ac.ma , [5]medvall@ju.edu.sa .

SPECIAL ISSUE ON:

The 1st International Conference on Sciences and Techniques for Renewable Energy and the Environment.
(STR2E 2025)
May 6-8, 2025 at FST-Al Hoceima-Morocco.

KEYWORDS

Artificial Neural Network, Maximum Power Point Tracking, Integral Sliding Mode Control.

ABSTRACT

Mitigating nonlinearities and parameter fluctuations in high-rated wind energy systems is crucial for efficient energy conversion and grid integration. This paper presents a robust Integral Sliding Mode Control (ISMC) strategy for monitoring active and reactive power in a DFIG-based wind turbine. An artificial neural network based MPPT algorithm enhances speed control and addresses power fluctuations. The proposed ISMC ensures an optimal dynamic response to wind variations. Its performance is compared using a PI controller in Field-Oriented Control (FOC_PI) in MATLAB/Simulink on a wind system of 1.5 MW and tested under real-wind conditions. Simulation results confirm that ISMC outperforms FOC_PI in reference tracking, accuracy, dynamic behavior, and current distortion reduction.

*Corresponding author.

DOI: https://doi.org/10.51646/jsesd.v14iSTR2E.894

التحكم المتين في أنظمة تحويل طاقة الرياح القائمة على المولد الحثي مزدوج التغذية مع تعقب نقطة القدرة القصوى المعتمد على الشبكات العصبية الاصطناعية

أشرف الوالي, ياسين لكحل, محمد بنشكرة, حميد شوجاع, محمد فال ولد محمد.

ملخص: يُعدّ التخفيف من اللاخطيات وتغيرات المعلمات في أنظمة طاقة الرياح ذات القدرة العالية أمرًا بالغ الأهمية لتحقيق تحويل فعال للطاقة والتكامل مع الشبكة. يقدم هذا البحث استراتيجية تحكم قوية تعتمد على التحكم بالانزلاق التكاملي (ISMC) لمراقبة القدرة الفعالة وغير الفعالة في توربينات الرياح المعتمدة على المولد غير المتزامن ذو التغذية المزدوجة (DFIG). يعزز خوارزمية التتبع الأقصى لنقطة القدرة (MPPT) القائمة على الشبكات العصبية الاصطناعية من التحكم في السرعة ويعالج تقلبات القدرة. يضمن التحكم بالانزلاق التكاملي (ISMC) استجابة ديناميكية مثلى لتغيرات الرياح. يتم مقارنة أدائه باستخدام متحكم PI في التحكم الموجه للحقل (FOC-PI-) في بيئة Matlab/Simulink على نظام رياح بقدرة 1.5 ميجاواط، وتم اختباره في ظروف رياح حقيقية. تؤكد نتائج المحاكاة أن ISMC يتفوق على FOC-PI في تتبع الإشارة المرجعية، والدقة، والسلوك الديناميكي، وتقليل تشوه التيار.

الكلمات المفتاحية – الشبكات العصبية الاصطناعية، تعقب نقطة القدرة القصوى، التحكم بالانزلاق المتكامل.

1. INTRODUCTION

The increasing global demand for electricity, the depletion of fossil fuel resources, and the escalating impacts of global warming have intensified the search for sustainable and renewable energy solutions such as wind and solar power [1,2,3].

Among these, Wind Energy Conversion Systems (WECS) have gained significant attention due to their ability to provide clean and efficient energy. However, the nonlinear and fluctuating nature of wind speed presents a major challenge in maximizing energy extraction, necessitating the implementation of advanced control strategies [4,5,6]. To enhance energy capture, this study proposes an intelligent neural network-based Maximum Power Point Tracking (MPPT) control method especially designed to optimize power extraction under varying wind conditions. Unlike conventional MPPT techniques, which may struggle with dynamic wind variations, the proposed method leverages artificial intelligence to improve response time, robustness, and overall efficiency [7,8,9].

Doubly-Fed Induction Generators (DFIGs) are widely employed in WECS due to their robustness, durability, and ability to independently control active and reactive power, even under variable wind speeds [10,11].

However, achieving optimal performance requires efficient control strategies to regulate stator-generated power while ensuring a unity power factor. Among nonlinear control techniques, Sliding Mode Control (SMC) has proven to be a powerful approach for enhancing system performance [12]. Despite its advantages, traditional SMC suffers from chattering, a major drawback caused by discontinuous control action. To address this issue, this work introduces an Integral Sliding Mode Control (ISMC) strategy, which significantly reduces chattering while maintaining high dynamic performance and robustness. The main contributions of this paper are summarized as follows:

- The development of an intelligent MPPT strategy based on neural networks, applied on a wind turbine model described in figure1 ensuring optimal power extraction from wind energy.
- The implementation of an enhanced ISMC approach for DFIG-based WECS, effectively mitigating chattering effects and improving system stability.
- A comparative analysis between traditional SMC and the proposed ISMC, demonstrating the

advantages of the improved control methodology through numerical simulations.
This paper is structured as follows: Section 2 presents the dynamic modeling of the wind energy conversion system; Section 3 describes the configuration of the control strategies; Section 4 discusses the simulation results, providing a comparative analysis of the different control approaches; and, finally, Section 5 sums up the research findings and highlights future research prospects.

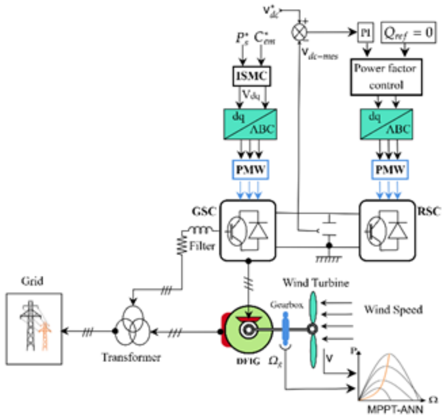

Figure 1. Diagrammatic Representation of the Studied System.

2. TURBINE MODEL

The wind turbine is characterized by the following expressions [2]:

$$P_t = \frac{1}{2}\rho\pi R^2 V^3 C_P(\lambda,\beta) \qquad (1)$$

In this work, the variations of Cp (λ,β) are modeled by the following equation.

$$\begin{cases} Cp(\lambda,\beta) = 0.5\left(\frac{116}{\lambda i} - 0.4\beta - 5\right)exp\left(\frac{-21}{\lambda i}\right) \\ \qquad + 0.0068\,\lambda \\ \frac{1}{\lambda i} = \frac{1}{\lambda + 0.08\beta} - \frac{0.035}{\beta^3+1} \quad ; \quad \lambda = \frac{\Omega_t R}{V} \end{cases} \qquad (2)$$

2.1. MPPT WITH SPEED CONTROL

Maximizing WECS output power and performance requires MPPT. Additionally, a speed controller regulates rotor speed by imposing the necessary electromagnetic torque. The MPPT method generates the reference torque, to maintain the angular speed near its setpoint. Figure 2 illustrates the MPPT strategy.

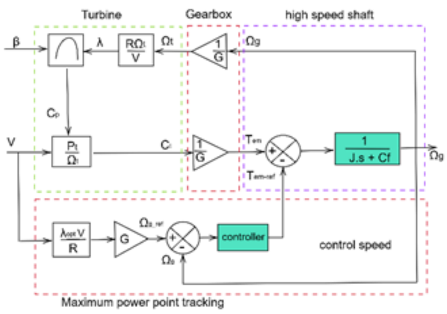

Figure 2. Integration of MPPT methodology.

2.2. ARTIFICIAL NEURAL NETWORKS (ANN)

The ANN model is inspired by the human brain, with interconnected neurons representing the nervous system. Each connection has a weight, similar to synapses. The study (detailed in Figure 3) uses a static Multi-Layer Perceptron (MLP) network, composed of input, hidden, and output layers arranged in a feed-forward style. The input layer processes sensor data, while hidden neurons are placed between the input and output layers.

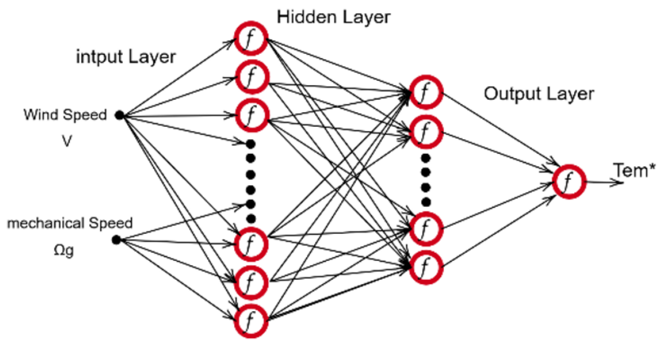

Figure 3. ANN Internal architecture.

3. DFIG MODEL

With respect to the dq Park reference frame, the DFIG's dynamic equations including the voltage equations, the flux equations, and the active and reactive powers' equations are defined by the equations (3) and (4), respectively, as follows [2,6]:

$$\begin{cases} V_{sd} = R_s i_{sd} + \dfrac{d}{dt}\phi_{sd} - \omega_s \phi_{sq} \\ V_{sq} = R_s i_{sq} + \dfrac{d}{dt}\phi_{sq} + \omega_s \phi_{sd} \\ V_{rd} = R_r i_{rd} + \dfrac{d}{dt}\phi_{rd} - (\omega_s - \omega_r)\phi_{rq} \\ V_{rq} = R_r i_{rq} + \dfrac{d}{dt}\phi_{rq} + (\omega_s - \omega_r)\phi_{rd} \end{cases} \quad (3)$$

$$\begin{cases} P_s = \dfrac{3}{2} Re\left\{\vec{V}_s \times \vec{I}_s^*\right\} = \dfrac{3}{2}\left(V_{sd} i_{sd} + V_{sq} i_{sq}\right) \\ Q_s = \dfrac{3}{2} Im\left\{\vec{V}_s \times \vec{I}_s^*\right\} = \dfrac{3}{2}\left(V_{sq} i_{sd} - V_{sd} i_{sq}\right) \end{cases} \quad (4)$$

4. SUGGESTED ISMC TECHNIQUE

Sliding Mode Control is a robust strategy known for its high efficiency and reliability in both transient and steady states, especially against system nonlinearities and disturbances [13,14]. It uses a discontinuous signal to drive the system to the sliding surface. However, the chattering phenomenon limits its use. This research develops an Integral Sliding Mode regulation technique to reduce chattering and regulate powers of DFIG [15].
The state representation of the DFIG is given by the equations:

$$\dot{X} = f(x,t) + g(x,t)u \tag{5}$$

$$f(x,t) = \begin{bmatrix} -\frac{R_r}{(\sigma L_r)^2}\left(\sigma L_r i_{rd} + \frac{MV_{sq}}{\omega_s L_S}\right) + \frac{R_r M \psi_{sd}}{L_S(\sigma L_r)^2} \\ +\frac{\omega_r}{\sigma L_r}\left(\sigma L_r i_{rq} + \frac{M}{\omega_s L_s} V_{sd}\right) \\ -\frac{R_r}{(\sigma L_r)^2}\left(\sigma L_r i_{rq} + \frac{MV_{sd}}{\omega_s L_s}\right) \\ +\frac{R_r M \psi_{sq}}{L_s(\sigma L_r)^2} + \frac{\omega_r}{\sigma L_r}\left(\sigma L_r i_{rd} + \frac{M}{\omega_s L_s} V_{sq}\right) \end{bmatrix} \tag{6}$$

$$g(x,t) = \begin{bmatrix} \frac{1}{\sigma L_r} & 0 \\ 0 & \frac{1}{\sigma L_r} \end{bmatrix} \tag{7}$$

Where : $X = \begin{bmatrix} i_{rd} & i_{rq} \end{bmatrix}$

$$\begin{cases} S_d = e_d(t) + \alpha_d e_I(t) \\ S_q = e_q(t) + \alpha_q e_I(t) \end{cases} \tag{8}$$

$$\begin{cases} \dot{S}_d = \dot{e}_d(t) + \alpha_d \dot{e}_I(t) = 0 \\ \dot{S}_q = \dot{e}_q(t) + \alpha_q \dot{e}_I(t) = 0 \end{cases} \tag{9}$$

$$\begin{cases} \dot{i}_{rd} - \dot{i}_{rd-ref} + \alpha_d \dot{e}_I(t) = 0 \\ \dot{i}_{rq} - \dot{i}_{rq-ref} + \alpha_q \dot{e}_I(t) = 0 \end{cases} \tag{10}$$

$$\begin{bmatrix} U_{rd} \\ U_{rq} \end{bmatrix} = g^{-1} \begin{bmatrix} \dot{i}_{rd-ref} - f_1 - \alpha_d sign(e_d(t)) \\ \dot{i}_{rq-ref} - f_2 - \alpha_q sign(e_q(t)) \end{bmatrix} \tag{11}$$

$$V = \frac{1}{2} S_{dq}^T S_{dq} \tag{12}$$

The derivative of (12) yields:

$$\dot{V} = \frac{S_d}{\sigma L_r}\left(\dot{i}_{rd-ref} - f_1 - \alpha_d sign(e_d(t))\right)$$

$$+\frac{S_q}{\sigma L_r}\left(\dot{i}_{rq-ref} - f_2 - \alpha_q sign(e_q(t))\right)$$

$$+\frac{S_q}{\sigma L_r}\gamma_q-\frac{S_q}{\sigma L_r}\alpha_q sign\left(e_q\left(t\right)\right) \qquad (13)$$

$$+\frac{S_q}{\sigma L_r}\gamma_q-\frac{S_q}{\sigma L_r}\alpha_q sign\left(e_q\left(t\right)\right) \qquad (13)$$

5. RESULTS AND DISCUSSIONS

The simulation evaluation of this sub-section employs a 1.5 MW DFIG model-based wind turbine. Figure 4 shows the simulated wind speed profile, which ranges from 7 to 9 m/s. Figures 5 and 6 show real-time variations of the power coefficient and TSR. At a 0° angle β, the power coefficient reaches its optimal value of 0.477, corresponding to the optimal TSR of λopt =8.14. Figure 7 shows that the ANN-MPPT controller keeps the DFIG's rotor speed close to the critical synchronous speed, following real-time data with no overshoot, demonstrating efficient and effective control under hyper- and hypo-synchronous conditions.

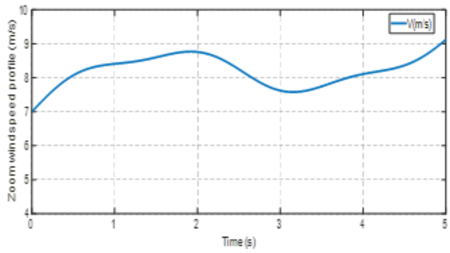

Figure 4. Wind speed

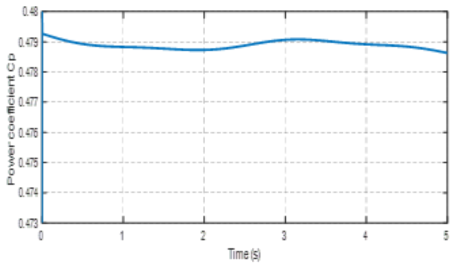

Figure 5. Coefficient Cp

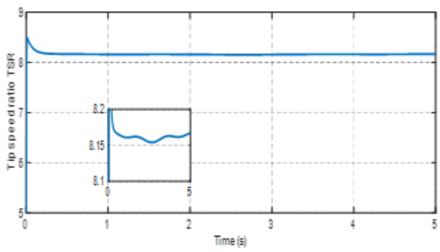

Figure 6. TSR

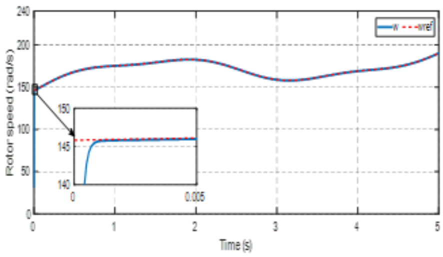

Figure 7. Rotor speed

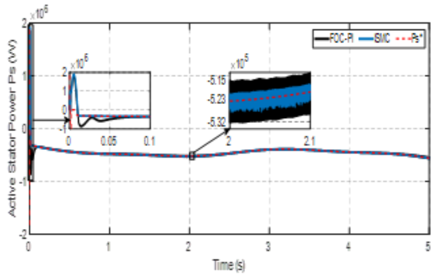

(a)

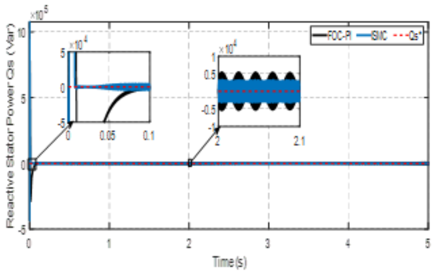

(b)

Figure 8. Stators Powers: (a) Ps, (b) Qs

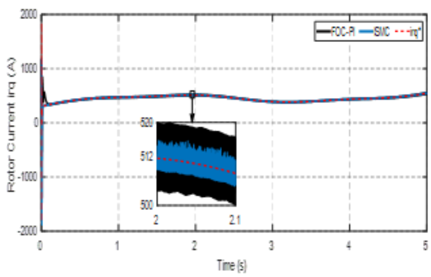

(a)

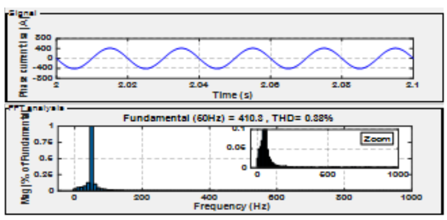

(a)

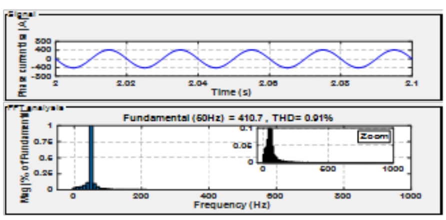

(b)

Figure 10. THD: (a) FOC_PI and (b) ISMC.

Figures 10(a) and 10(b) display the THD spectral analysis of the stator current for the 'a' phase, comparing the FOC_PI and ISMC controllers. Using FFT for frequency domain analysis, the FOC_PI shows a THD of 0.91%, while the ISMC significantly reduces it to 0.38%, demonstrating that the ISMC effectively minimizes current harmonics.

Table 1. Evaluation of FOC_PI vs adaptive ISMC.

Performance	FOC used PI	ISMC
Response time (s)	0.403	0.294
THD i_sa (%)	0.91	0.38
Rise time (s)	0.268	0.196
Set point tracking	Good	Very Good

Table 1 compares the ISMC and FOC_PI in terms of static error, response time, THD of Isa current, and set-point tracking, showing significant improvements with the ISMC, including reduced harmonics, minimal static errors, faster response, and better set-point accuracy. This makes it suitable for the field of wind turbines [16].

6. CONCLUSION

This study introduces the DFIG and turbine model. It implements an MPPT strategy with an ANN-based speed controller, which efficiently tracks peak power. ISMC and FOC_PI controllers are applied to regulate the DFIG's power flow components, with simulation results showing that ISMC outperforms FOC_PI in accuracy, reduced current distortion, improved dynamics, and better reference tracking. Using FFT for frequency domain analysis, the FOC_PI shows a THD of 0.91%, while the ISMC significantly reduces it to 0.38%, demonstrating that the ISMC effectively minimizes current harmonics. This makes it suitable for analyzing dynamic instabilities in wind energy generation.

Authors contribution: Achraf El Ouali : Conceptualization, Data collection, Writing – original draft. Yassine Lakhal : Supervision Writing – review & editing. Mohamed Benchagra : Formal analysis, Writing – review & editing. Hamid Chojaa : Formal analysis, Conceptualization, Writing – original draft, Methodology, Supervision. Mohamed Vall O. Mohamed : review & editing.
Funding: The authors are warmly grateful to the support of "The Moroccan Association of Sciences and Techniques for Sustainable Development (MASTSD), Beni Mellal, Morocco.
Data Availability Statement: The data that support the findings of this study are available from the corresponding au-thor upon reasonable request.
Conflicts of Interest: The authors declare no conflicts of interest.
Acknowledgements: The authors would like to thank the organizers of the 1st International Conference on Sciences and Techniques for Renewable Energy and the Environment, held from May 6th to 8th, 2025, at the Faculty of Sciences and Techniques, Al Hoceima, Morocco, for their valuable support and insightful discussions during this research.

REFERENCES

[1] H. Chojaa, A. Derouich, O. Zamzoum, A. Watil, M. Taoussi, A. Y. Abdelaziz, Z. M. Salem Elbarbary, and M. A. Mossa, "Robust Control of DFIG-Based WECS Integrating an Energy Storage System With Intelligent MPPT Under a Real Wind Profile," IEEE Access, vol. 11, pp. 90065–90083, 2023, doi: 10.1109/ACCESS.2023.3306722.

[2] Y. Sahri, S. Tamalouzt, F. Hamoudi, S. Lalouni, and M. Bajaj, "New intelligent direct power control of DFIG-based wind conversion system by using machine learning under variations of all operating and compensation modes," Energy Reports, vol. 7, pp. 6394–6412, 2021, doi: 10.1016/j.egyr.2021.09.042.

[3] Y. Lakhal, M. Haiek, F. Z. Baghli, Y. Ait El Kadi, M. Benchagra, and D. Sarsri, "Smart flow control of an airfoil with trailing edge flap for wind turbines using a fuzzy logic strategy," International Journal on Energy Conversion (IRECON), vol. 12, no. 5, p. 195, 2024, doi: 10.15866/irecon.v12i5.25100.

[4] I. Sami, S. Ullah, Z. Ali, N. Ullah, and J.-S. Ro, "A Super Twisting Fractional Order Terminal Sliding Mode Control for DFIG-Based Wind Energy Conversion System," Energies, vol. 13, no. 9, 2020, doi: 10.3390/en13092158.

[5] Y. Djeriri, A. Meroufel, and A. Massoum, "Artificial neural network based direct torque control of doubly fed induction generator," International Journal of Electrical Power & Energy Systems, vol. 49, pp. 234–242, 2013, doi: 10.1016/j.ijepes.2012.12.019.

[6] J. Bhukya, "Enhancing power system stability in wind-integrated networks through coordinated fuzzy logic control of PSS and POD for sustainable energy futures," International Journal of Ambient Energy, vol. 45, no. 1, 2024, doi: 10.1080/01430750.2024.2391096.

[7] M. Fdaili, A. Essadki, and T. Nasser, "Comparative analysis between robust SMC & conventional PI controllers used in WECS based on DFIG," International Journal of Renewable Energy Research (IJRER), vol. 7, no. 4, pp. 1795–1803, 2017, doi: 10.20508/ijrer.v7i4.6441.g7267.

[8] S. Karthikeyan, C. Ramakrishnan, "A hybrid fuzzy logic-based MPPT algorithm for PMSG-based variable speed wind energy conversion system on a smart grid," Energy Storage and Saving, Volume 3, Issue 4, Pages 295-304, 2024, doi : 10.1016/j.enss.2024.08.001.

[9] A. El Ouali, Y. Lakhal, M. Benchagra, H. Chojaa, and S. Samagassi, "Evaluating the impact of drivetrain vibrations on MPPT control performance in horizontal axis wind turbines," E3S Web of Conferences, vol. 582, p. 03001, 2024, doi: 10.1051/e3sconf/202458203001.

[10] A. Zanelli, J. Kullick, H. Eldeeb, G. Frison, C. Hackl, and M. Diehl, "Continuous Control Set Nonlinear Model Predictive Control of Reluctance Synchronous Machines," arXiv preprint arXiv:1910.10681, 2019.

[11] G. Han, L. Zhang, D. Wang, and X. Zhao, "Speed synchronization control of dual-SRM drive with ISMC-based cross coupling control strategy," IEEE Transactions on Transportation Electrification, vol. 9, no. 2, pp. 2524–2534, 2023, doi: 10.1109/TTE.2022.3208230.

[12] R. Subramaniam and Y. H. Joo, "Passivity-based fuzzy ISMC for wind energy conversion systems with PMSG," IEEE Transactions on Systems, Man, and Cybernetics: Systems, vol. 51, no. 4, pp. 2212–2220, 2021, doi: 10.1109/TSMC.2019.2930743.

[13] S. Rajendran, D. Jena, M. Diaz, J. Rodriguez, " Design of modified complementary terminal sliding mode controller for wind turbine at region II using a two-mass model, " Results in Engineering, Volume 24, 103026, ISSN 2590-1230, 2024, doi: 10.1016/j.rineng.2024.103026.

[14] L. Xiong, P. Li, M. Ma, Z. Wang, and J. Wang, "Output power quality enhancement of PMSG with fractional order sliding mode control," International Journal of Electrical Power & Energy Systems, vol. 115, p. 105402, 2020, doi: 10.1016/j.ijepes.2019.105402.

[15] S. Hassan, B. Abdelmajid, Z. Mourad, S. Aicha, and B. Abdennaceur, "PSO-Backstepping controller of a grid connected DFIG based wind turbine," International Journal of Electrical and Computer Engineering, vol. 10, no. 1, pp. 856–867, 2020, doi: 10.11591/ijece.v10i1.pp856-867.